
Research Articles: Cellular/Molecular

Activating Transcription Factor 4 (ATF4) regulates neuronal activity by controlling GABA_BR trafficking

Carlo Corona¹, Silvia Pasini¹, Jin Liu¹, Fatou Amar¹, Lloyd A Greene¹ and Michael L Shelanski¹

¹*Department of Pathology & Cell Biology and the Taub Institute for Research on Alzheimer's Disease and the Aging Brain, Columbia University Medical Center, New York, NY, 10033*

DOI: 10.1523/JNEUROSCI.3350-17.2018

Received: 27 November 2017

Revised: 29 May 2018

Accepted: 31 May 2018

Published: 6 June 2018

Author contributions: M.S. and L.A.G. designed research; M.S. and L.A.G. wrote the paper; C.C., S.P., J.L., and F.A. performed research; C.C., S.P., J.L., and F.A. analyzed data.

Conflict of Interest: The authors declare no competing financial interests.

We thank Drs. Ottavio Arancio and Asa Abeliovich for providing equipment for electrophysiological experiments. This work was supported in part by grants from the NIH-NINDS (R01NS033689 and R01NS072050), by the Taub Institute for Research in Alzheimer's disease and by the Marilyn and Henry Taub Foundation.

Corresponding author: Michael L Shelanski, mis7@columbia.edu

Cite as: J. Neurosci ; 10.1523/JNEUROSCI.3350-17.2018

Alerts: Sign up at www.jneurosci.org/cgi/alerts to receive customized email alerts when the fully formatted version of this article is published.

Accepted manuscripts are peer-reviewed but have not been through the copyediting, formatting, or proofreading process.

Copyright © 2018 the authors

1 **Title:** Activating Transcription Factor 4 (ATF4) regulates neuronal activity by controlling GABA_BR
2 trafficking

3 **Abbreviated title:** ATF4 regulates neuronal excitability via GABA_BRs

4 **Author names and affiliation:** Carlo Corona¹, Silvia Pasini^{1,2}, Jin Liu¹, Fatou Amar¹, Lloyd A
5 Greene¹, and Michael L Shelanski¹

6 ¹ Department of Pathology & Cell Biology and the Taub Institute for Research on Alzheimer's
7 Disease and the Aging Brain, Columbia University Medical Center, New York, NY, 10033

8 ² Present address: Department of Ophthalmology and Visual Science, Vanderbilt University
9 Medical Center, Nashville, TN

10 **Corresponding author:** Michael L Shelanski, mls7@columbia.edu

11 **Number of pages:** 16

12 **Number of figures:** 7

13 **Number of words:** Abstract=250, Introduction=509, and Discussion=1140

14 **Conflict of Interest:** Authors declare no conflict of interests

15 **Acknowledgements:** We thank Drs. Ottavio Arancio and Asa Abeliovich for providing equipment
16 for electrophysiological experiments. This work was supported in part by grants from the NIH-
17 NINDS (R01NS033689 and R01NS072050), by the Taub Institute for Research in Alzheimer's
18 disease and by the Marilyn and Henry Taub Foundation.

19

20 **ABSTRACT**

21 Activating Transcription Factor 4 (ATF4) has been postulated as a key regulator of learning and
22 memory. We previously reported that specific hippocampal ATF4 down-regulation causes deficits
23 in synaptic plasticity and memory and reduction of glutamatergic functionality. Here we extend
24 our studies to address ATF4's role in neuronal excitability. We find that long-term ATF4
25 knockdown in cultured rat hippocampal neurons significantly increases the frequency of
26 spontaneous action potentials. This effect is associated with decreased functionality of
27 metabotropic GABA_B receptors (GABA_BRs). Knocking down ATF4 results in significant reduction
28 of GABA_BR-induced GIRK-currents and increased mIPSCs frequency. Furthermore, reducing
29 ATF4 significantly decreases expression of membrane-exposed, but not total, GABA_BR 1a and
30 1b subunits, indicating that ATF4 regulates GABA_BR trafficking. In contrast, ATF4 knockdown has
31 no effect on surface expression of GABA_BR2s, several GABA_BR-coupled ion channels or β 2 and
32 γ 2 GABA_ARs. Pharmacologic manipulations confirmed the relationship between GABA_BR
33 functionality and action potential frequency in our cultures. Specifically, the effects of ATF4 down-
34 regulation cited-above are fully rescued by transcriptionally active, but not by transcriptionally-
35 inactive, shRNA-resistant, ATF4. We previously reported that ATF4 promotes stabilization of the

36 actin-regulatory protein Cdc42 by a transcription-dependent mechanism. To test the hypothesis
37 that this action underlies the mechanism by which ATF4 loss affects neuronal firing rates and
38 GABA_BR trafficking, we down-regulated Cdc42 and found that this phenocopies the effects of
39 ATF4 knockdown on these properties. In conclusion, our data favor a model in which ATF4, by
40 regulating Cdc42 expression, affects trafficking of GABA_BRs, which in turn modulates the
41 excitability properties of neurons.

42

43 **Significance statement:** GABA_B receptors (GABA_BRs), the metabotropic receptors for the
44 inhibitory neurotransmitter GABA, have crucial roles in controlling the firing rate of neurons.
45 Deficits in trafficking/functionality of GABA_BRs have been linked to a variety of neurological and
46 psychiatric conditions, including epilepsy, anxiety, depression, schizophrenia, addiction, and pain.
47 Here we show that GABA_BRs trafficking is influenced by Activating Transcription Factor 4 (ATF4),
48 a protein that has a pivotal role in hippocampal memory processes. We found that ATF4 down-
49 regulation in hippocampal neurons reduces membrane-bound GABA_BR levels and thereby
50 increases intrinsic excitability. These effects are mediated by loss of the small GTPase Cdc42
51 following ATF4 down-regulation. These findings reveal a critical role for ATF4 in regulating the
52 modulation of neuronal excitability by GABA_BRs.

53

54 **Introduction**

55 Normal cognitive functions rely on the balance of neuronal excitability properties throughout the
56 brain as well as on synaptic plasticity (Beck and Yaari, 2008). Among the many proteins reported
57 to influence cognition, mounting evidence suggests a pivotal role for Activating Transcription
58 Factor 4 (ATF4), an ubiquitously expressed member of the ATF/CREB transcription factor family
59 of basic leucine zipper proteins. In addition to its well-known functions as a stress-induced protein
60 (Ameri and Harris, 2008), a number of studies have implicated ATF4 in synaptic plasticity and in
61 learning and memory. Depending on cellular context, ATF4 has been characterized as either an
62 inhibitor or promoter of synaptic plasticity (Pasini et al., 2015). Similarly divergent suggestions
63 about ATF4's functions in learning and memory have been advanced, but these are largely based
64 on indirect and non-selective manipulation of ATF4 activity or expression (Chen et al., 2003;
65 Costa-Mattioli et al., 2007). To probe directly ATF4's role in normal brain function, we have
66 monitored the consequences of its knockdown or knockout in neuronal culture and in animals.
67 This has led to observations that ATF4 plays a role in regulation of mushroom dendritic spine
68 density as well as in synaptic glutamatergic function (Liu et al., 2014). These effects appeared to
69 be due to ATF4's direct transcriptional regulation of RhoGDI α (product of the *Arhgdia* gene), which
70 in turn affects stability of the Rho family member Cdc42 that is involved in regulation of the actin
71 cytoskeleton (Pasini et al., 2016). At the physiological level, loss of ATF4 manifested in reduced
72 frequency and amplitude of mEPSCs, followed by defective LTP and LTD as well as in memory
73 deficits (Pasini et al., 2015). Of relevance, similar deficiencies in plasticity and memory have been
74 observed after conditional Cdc42 knockout in brain (Kim et al., 2014). In the context of ATF4's
75 role in neuronal functionality, one area of interest is in its relation to GABA_B receptors (GABA_BRs),
76 the G-protein-linked metabotropic receptors for the inhibitory neurotransmitter GABA. Several

77 studies have shown direct association of GABA_BRs with ATF4 (Nehring et al., 2000; White et al.,
78 2000; Vernon et al., 2001; Ritter et al., 2004) while another study reported that ATF4 differentially
79 regulates activity of promoters for the GABA_BRs subunits 1a and 1b (Steiger et al., 2004).
80 GABA_BRs are widely expressed in brain and regulate neuronal excitability by modulating activity
81 of G protein-gated inwardly rectifying K⁺ channels (GIRKs), voltage-gated Ca²⁺ channels and
82 adenylyl cyclase (Gassmann and Bettler, 2012). Activation of GABA_BRs has been reported to
83 hyperpolarize and decrease the threshold, while deactivation of the receptors increases the
84 threshold required to generate an action potential (Ladera et al., 2008). Thus, alterations of
85 GABA_BR trafficking/functionality have the potential to significantly alter intrinsic neuronal
86 excitability and brain function. In this work, we have investigated the role of ATF4 in neuronal
87 excitability. We find that ATF4 knockdown in cultured hippocampal neurons significantly increases
88 their firing rate and that this appears to be due to reduced trafficking of GABA_BR to the cell surface.
89 These effects in turn appear to be a consequence of ATF4's regulation of Cdc42 stability.

90 **Methods**

91 Cell cultures

92 Primary hippocampal cultures were prepared as previously described (Liu et al., 2015). Briefly,
93 hippocampi were dissected from E18 rat embryos of either sex and, after dissociation, neurons
94 were plated on poly-D-lysine-coated 12-well-plates at the density of 3×10^5 cells/well. Neurons
95 were maintained in Neurobasal medium (Invitrogen) supplemented with 2% B-27 (Invitrogen) and
96 0.5 mM glutamine (Invitrogen). Elisa measurements of both cell media and cell lysates revealed
97 the presence of both GABA and glutamate in the culture (glutamate=32.2 μ g, GABA=13.9 μ g).

98

99 DNA constructs, lentivirus preparation and infection

100 All shRNAs were cloned in the pLVTHM vector (Addgene), which contains an EF-1 α promoter for
101 target gene expression, using the following oligo DNA pairs as previously described (Liu et al.,
102 2014).

103 Lenti-shRNA control:

104 5'-CGCGTCACAGCCCTTCCACCTCCATTCAAGAGATGGAGGTGGAAGGGCTGTGTTTTTT

105 A-3' and 5'-CGCGTAAAAAACACAGCCCTTCCACCTCCATCTCTTGAATGGAGGTGGA
106 AGGGCTGTGA-3'.

107 Lenti-shATF4:

108 5' -CGCGTGCCTGACTCTGCTGCTTATTTCAAGAGAATAAGCAGCAGAGTCAGGC

109 TTTTTTA-3' and 5' -CGCGTAAAAAAGCCTGACTCTGCTGCTTATTCTCTTGAA

110 ATAAGCAGCAGAGTCAGGCA-3'

111 Lenti-shATF4 addback was generated using the QuickChange Site-directed Mutagenesis kit
112 (Stratagene). Point mutations were introduced into the Lenti-ATF4 at the recognition site for
113 shATF4 (CCTGACTCTGCTGCTTAT to CCAGAGTCAGCTGCTTAC).

114 Lenti-shATF4 mut/addback was generated from shATF4addback by introducing point mutations
115 at the DNA binding site (292RYRQKKR298 to 292GYLEAAA298).

116 Lenti-shCdc42 was generated according to a published siRNA sequence 5'-
117 GAUAACUCACCACUGUCCATT-3' (Deroanne et al., 2005). A scrambled shRNA (lenti-
118 shCdc42scr) was generated by using the following oligo DNA pair: 5'-
119 CGCGTGTCCAACGTCCATATACCATTCAAGAGATGGTATATGGACGTTGGACTTTTTTA-3'
120 and 5'-CGCGTAAAAAAGTCCAACGTCCATATACCATCTCTTGAATGGTATATGGACGTTG G
121 ACA-3'. Lentiviral particles were produced using the 2nd generation packaging system. Briefly,
122 HEK293T cells were transfected with the respective lentiviral constructs for shRNA together with
123 the packaging vectors psPAX2 and pMD2.G (Addgene) using calcium phosphate. Two and three
124 days after transfection, cell supernatants were collected and lentiviral particles were concentrated
125 20–30x by centrifugation in Amicon Ultra centrifugal filters (100KD) (Millipore). Viral titer ranged
126 between 1–5×10⁶ virions/μl. Primary neuronal cultures were infected with viral particles on *Day In*
127 *Vitro* 7 (*DIV*7) and RNA and protein extraction were performed at the indicated time points.

128

129 RNA Extraction and Quantitative RT-PCR

130 Total RNA was extracted from rat primary hippocampal cultures 4, 8, and 12 days after lentiviral
131 infection according to the RNeasy Mini Protocol (Quiagen kit). RNA concentration and purity were
132 determined using a NanoDrop 8000 (Thermo Scientific, Wilmington, DE). mRNA was then
133 reverse-transcribed into cDNA using the 1st Strand cDNA Synthesis System for quantitative RT-
134 PCR (Origene) following the manufacturer's instructions. Reaction mixtures were diluted 5-fold
135 and subjected to qRT-PCR amplification (Eppendorf) using FastStart SYBR Green Master mix
136 (Roche). The following primers were used: ATF4: F 5'-ATGCCAGATGAGCTCTTGACCAC-3' and
137 R 5' -GTCATTGTCAGAGGGAGTGTCTTC-3'; αTubulin: F 5'-TACACCATTGGCAAGGAGAT-3'
138 and R 5'-GGCTGGGTAAAT GGAGAACT-3; GABA_BR 1a: F 5'-CACACCCAGTCGCTGTG-3' and
139 R 5'-GAGGTCCCCACCCGTCA-3'; GABA_BR 1b 5'-GGGACCCTGTACCCCGGTG-3' and R 5'-
140 GGAGTGAGAGGCCACACC-3'. Relative product quantities for each transcript were performed
141 in triplicate, normalized to αTubulin mRNA as an endogenous control, and determined using the
142 comparative CT method.

143

144 Electrophysiology

145 Primary hippocampal neurons (19-21 *DIV*, 2 weeks after lentiviral infection) were used for tight
146 seal conventional whole-cell patch clamp. All the currents were recorded from pyramidal-like
147 neurons, based on their large (~15μm) triangular shaped somas. Coverslips were placed in a
148 recording chamber with bath solution containing (in mM): 119 NaCl, 5 KCl, 20 Hepes, 30 glucose,
149 2 CaCl₂, 2 MgCl₂. The pH and osmolarity of the bath solution were adjusted to 7.3 and 330

150 mOsm/L, respectively. For spontaneous action potential recordings, glass pipettes were filled with
151 intracellular electrode solution (pH 7.3, 285 mOsm/L) containing (in mM): 130 K-gluconate, 10
152 KCl, 10 HEPES, 1 MgCl₂, 0.06 CaCl₂, 0.1 EGTA, 3 MgATP, 0.3 Na₂GTP, and typically registered
153 4–8 MΩ pipette resistances. Following acquisition of electrical access, cells were held in current-
154 clamp mode at I=0. For mIPSCs experiments, glass pipettes were filled with intracellular electrode
155 solution (pH 7.3, 285 mOsm/L) containing (in mM): 130 KCl, 10 Hepes, 0.5 CaCl₂, 1 EGTA, 3
156 MgATP, 0.3 Na₂GTP. Furthermore, 1 μM TTX, 10 μM CNQX, and 50 μM D-APV were
157 continuously perfused during the experiment. All the cells were recorded at -70 mV for 10 min
158 and a 5 mV hyperpolarizing test pulse was applied periodically during recordings to ensure that
159 the access resistance did not change significantly and was less than 25 MΩ. If not, the recordings
160 were discarded. Signals were filtered at 2 kHz, digitized at 10 kHz, stored and analyzed offline
161 using MiniAnalysis Software (Synaptosoft, Version 6.0.7). The threshold for event detection was
162 set at 5 pA. Recordings were performed at room temperature under constant perfusion (2 mL/min)
163 and acquired using Clampex software and a microamplifier (MultiClamp 700B, Molecular
164 Devices). For Baclofen-induced GIRK currents, hippocampal neurons were bathed initially with a
165 solution containing (in mM) 119 NaCl, 5 KCl, 20 Hepes, 30 glucose, 2 CaCl₂, 2 MgCl₂ (pH 7.3,
166 330 mOsm/L) and then switched to a high potassium solution (hK) containing (in mM) 85 NaCl,
167 60 KCl, 2 MgCl₂, 2 CaCl₂, 10 Hepes, 10 Glucose (pH 7.3) to determine the amplitude of the basal
168 potassium current. When the basal current reached equilibrium, Baclofen diluted in hK
169 was applied. The hK induced current was subtracted from the total current to obtain the Baclofen-
170 induced GIRK current. Membrane potential was held at -70 mV throughout the duration of the
171 experiment.

172 Surface and total protein isolation

173 Membrane-bound and total protein isolation was conducted using the EZ-Link NHS-PEO4-
174 Biotinylation Kit (Pierce), following manufacturer's instructions. Briefly, cells were gently washed
175 three times with ice-cold PBS containing 1 mM MgCl₂ and 0.1 mM CaCl₂ (PBS/CM) and then
176 incubated with 500 μg/ml of EZ-link NHS-PEO4-biotin dissolved in ice-cold PBS at 4°C for 1 hour.
177 Cells were then washed once with ice-cold PBS and the reaction quenched by adding 500 μl of
178 100 mM glycine for 10 minutes, followed by 3 washes in ice-cold-PBS. Cells were then harvested
179 in RIPA buffer supplemented with protease/phosphatase inhibitor and centrifuged at 14000 rpm
180 for 15 minutes at 4°C. 30 μl of the resulting supernatant were collected for total protein input and
181 the rest incubated with 50 μg of streptavidin beads, rotating overnight at 4°C. Beads were washed
182 5 times with RIPA buffer and bound proteins eluted with 1x sample buffer by boiling for 5 minutes.

183 Immunoblotting

184 After adding NuPAGE LDS Sample Buffer (Invitrogen) and 5% β-mercaptoethanol, samples were
185 boiled for 15 min and proteins were separated by electrophoresis on 4-12% BisTris SDS-
186 acrylamide gels (Invitrogen). After transfer, the membranes were blocked for 1 hour at room
187 temperature with 5% milk and then incubated overnight with primary antibody. The following
188 primary antibodies were used: rabbit anti-GABA_B R1 (1:1000, Abcam, #55051 (Zapata et al.,
189 2017)), GABA_B R2 (1:1000, Cell Signaling, #3839), rabbit anti-GABA_AR β2 (1:1000, Synaptic
190 Systems, #224803), rabbit anti-GABA_AR γ2 (1:1000, Synaptic Systems, #224003), rabbit anti-

191 ATF4 (1:1000, Cell Signaling, #11815), rabbit anti-Cdc42 (1:1000, Cell Signaling, #2462S), rabbit
192 anti-GIRK1 (1:500, Abcam, #129182), rabbit anti-GIRK2 (1:200, Sigma-Aldrich, #P8122), rabbit
193 anti-GIRK3 (1:400, Sigma-Aldrich, #P8247), mouse anti-GAPDH (1:10000, Invitrogen, #MA1-
194 16757), rabbit anti-K_v1.1 (1:400, Sigma-Aldrich, #P8247), mouse anti-K_v2.1 (1:500, Abcam,
195 #ab192761), rabbit anti-K_v4.2 (1:200, Sigma-Millipore, #07-491), rabbit anti-Ca_v2.1 (1:500,
196 abcam, #ab32642). Densitometric quantification of the bands was performed using ImageJ
197 software (NIH). Total level of proteins (input) was normalized to GAPDH, while membrane-bound
198 samples were normalized with the ratio input/GAPDH. GAPDH was undetectable in the
199 membrane-bound fraction, therefore excluding the possibility that the membrane was leaky or
200 compromised.

201 Statistical analysis

202 Data are shown as means \pm SEM. Comparison between two groups was performed with a two-
203 tailed unpaired Student's t test. Comparison between multiple groups was performed using two-
204 way ANOVA, followed by a Bonferroni *post hoc* test when applicable. Statistical significance was
205 set at $p < 0.05$.

206

207 Results

208

209 ATF4 knockdown increases neuronal excitability

210 We previously described a key role for ATF4 in modulating glutamatergic neurotransmission both
211 *in vitro* and *in vivo* and in regulating dendritic spines (Liu et al., 2014; Pasini et al., 2015). Given
212 the pivotal roles of these two aspects in controlling the excitability properties of neurons, we next
213 set out to directly investigate the role of ATF4 in intrinsic neuronal excitability. For this purpose,
214 we used lentivirally delivered shRNAs to specifically down-regulate ATF4 expression in 7 DIV
215 cultured rat hippocampal neurons and performed whole-cell patch-clamp two weeks after the
216 infection to record the frequency of spontaneously-occurring action potentials (sAPs). At this time
217 in culture (3 weeks total), the neurons have formed extensive synaptic connections (Liu et al.,
218 2014). As shown in Figure 1A,B, knockdown of ATF4 resulted in an approximately 3-fold increase
219 in the frequency of sAPs compared to neurons infected with a control shRNA
220 (shCtrl=0.35 \pm 0.07Hz, shATF4=1.11 \pm 0.26Hz; *post hoc* Bonferroni, shCtrl vs shATF4 $p < 0.01$) To
221 confirm that this result was not due to off-target effects, we performed a rescue experiment in
222 which the neurons were co-infected with lentiviruses expressing shATF4 and an ATF4 construct
223 (ATF4add) conservatively mutated to make it unresponsive to shATF4. This resulted in
224 knockdown of endogenous and overexpression of exogenous ATF4, respectively (Liu et al.,
225 2014). Our results indicate that ATF4add restored the firing rate to the control level (Fig. 1A,B;
226 shATF4+ATF4add=0.46 \pm 0.07Hz; *post hoc* Bonferroni, shCtrl vs shATF4+ATF4add, $p > 0.05$).
227 However, while ATF4 over-expression rescued the firing rate, it did not reduce it below that seen
228 in control cultures. Next, to test whether the effects of ATF4 on sAP frequency requires its
229 transcriptional activity, we co-infected cultured hippocampal neurons with shATF4 and a mutant

230 ATF4 construct, ATF4add/mut, that is not recognized by shATF4 and that encodes a mutant ATF4
231 that does not bind DNA and thus is transcriptionally inactive. This results in knockdown of
232 endogenous ATF4 and overexpression of inactive exogenous ATF4 (Liu et al., 2014). In contrast
233 to ATF4add, ATF4add/mut failed to rescue the effect of ATF4 knockdown (Fig. 1A,B;
234 shATF4+ATF4add/mut=1.17±0.21Hz; *post hoc* Bonferroni, shCtrl vs shATF4+ATF4add/mut,
235 $p<0.01$), suggesting that ATF4 must retain its transcriptional capability to regulate the frequency
236 of neuronal firing. Because APs are generated by voltage-gated sodium (Na_v) and potassium (K_v)
237 channels (Bean, 2007), we investigated whether ATF4 down-regulation could affect the neuronal
238 firing rate by influencing these major AP constituents. However, our results show no differences
239 in either Na_v or K_v I-V curves obtained from shCtrl- or shATF4-infected hippocampal cultures (Fig.
240 1C-E), suggesting that ATF4 regulates neuronal excitability by a mechanism independent of
241 effects on Na_v or K_v .

242 **ATF4 regulates trafficking of GABA_BRs to the membrane**

243 Among the many proteins reported to modulate the excitability of neurons, we focused on GABA_B
244 receptors (GABA_BRs), the metabotropic (G-protein coupled) receptors for GABA. Postsynaptic
245 GABA_BRs induce a slow inhibitory postsynaptic current (sIPSC) by gating Kir-type K^+ -channels.
246 This in turn hyperpolarizes the membrane and shunts excitatory currents, thereby inhibiting
247 generation of action potentials (Leung and Peloquin, 2006). In this light, we confirmed that
248 blocking GABA_BR activity in our cultures increases the neuronal firing rate. As shown in Figure
249 2A, application of the specific GABA_BR antagonist CGP55845 (10 μM) produced a rapid 8-fold
250 rise (from about 0.4 to 3.2 Hz) of sAP frequency. Of potential relevance, ATF4 has been reported
251 to directly bind GABA_BRs as well as to differentially regulate promoter activity of the subunits 1a
252 and 1b of GABA_BRs (Steiger et al., 2004). We therefore first investigated whether ATF4 down-
253 regulation affects expression of GABA_BRs at the transcriptional level. To achieve this, we infected
254 cultured hippocampal neurons with either shATF4 or shCtrl for 4-15 days and then carried out
255 qRT PCR. As shown in Figure 2B, knockdown of ATF4 did not significantly affect the transcript
256 levels of either GABA_BR 1a or 1b subunits (ATF4, 4 days: shCtrl=100±7.1%, shATF4=19.1±2.4%,
257 t test $p<0.01$; ATF4, 8 days: shCtrl=100±3%, shATF4=11.6±2.8%, t test $p<0.01$; ATF4, 12 days:
258 shCtrl=100±4.19%, shATF4=9.47±1.63%, t test $p<0.01$).

259 Next we determined whether knocking down ATF4 would alter total or membrane- bound protein
260 expression of GABA_BRs. To achieve this, we performed biotinylation of plasma membrane
261 proteins on cultured hippocampal neurons with or without ATF4 knockdown (infected at 7 *DIV* for
262 2 weeks), isolated the biotinylated proteins on streptavidin-bound beads and carried out western
263 immunoblotting analysis for GABA_BR subunits 1a and 1b on both the input (total cell lysate) and
264 membrane fractions. Densitometric quantification from multiple experiments showed that ATF4
265 down-regulation did not affect total GABA_BR 1a and 1b protein levels (Fig. 2C), but significantly
266 decreased the levels of GABA_BR subunits 1a and 1b in the biotinylated membrane fraction (Fig.
267 2C; GABA_BR 1a: shCtrl=100±11.8%, shATF4=46.7±10.7%; *post hoc* Bonferroni test: shCtrl vs
268 shATF4 $p<0.01$; GABA_BR 1b: shCtrl=100±7.2%, shATF4=48.2±7.9%; *post hoc* Bonferroni test:
269 shCtrl vs shATF4 $p<0.01$) thus indicating a role for ATF4 in regulating GABA_BR trafficking, but not
270 overall expression.

271 To address the question of whether the effect of ATF4 on membrane trafficking of GABA_BRs
272 involves ATF4's transcriptional activity, we performed a rescue experiment as above and found
273 that ATF4add/mut, in contrast to ATF4add, failed to reverse the effects of ATF4 knockdown (Fig.
274 2C; GABA_BR 1a, shATF4+ATF4add=95.1±10.3%, shATF4+ATF4add/mut=39.8±8.2%; *post hoc*
275 Bonferroni test: shCtrl vs shATF4+ATF4add $p>0.05$, shATF4 vs shATF4+ATF4add $p<0.05$, shCtrl
276 vs shATF4+ATF4add/mut $p<0.01$. GABA_BR 1b, shATF4+ATF4add=110.5±12.7%,
277 shATF4+ATF4add/mut=55.2±10%; *post hoc* Bonferroni test: shCtrl vs shATF4+ATF4add $p>0.05$,
278 shATF4 vs shATF4+ATF4add $p<0.001$, shCtrl vs shATF4+ATF4add/mut $p<0.05$). This indicates,
279 as with neuronal excitability, that ATF4 has a transcriptional role in regulating trafficking of
280 GABA_BRs. The data also show, as with excitability, that ATF4 over-expression is not sufficient to
281 drive surface expression of GABA_BRs beyond that seen with basal endogenous expression.

282 We next asked whether knocking down ATF4 might produce a more general or non-specific effect
283 on membrane proteins. Interestingly, both the total and membrane-bound levels of GABA_BR 2
284 (biotin labeled as above) were unaffected by ATF4 down-regulation (Fig. 2D). We also examined
285 the effect of shATF4 on membrane-exposed $\beta 2$ and $\gamma 2$ subunits of GABA_A receptors and found
286 no effects on either the total or membrane-exposed protein levels (Fig. 3A). In addition to
287 GABA_BRs, a wide variety of voltage-sensitive K and Ca channels has been described to regulate
288 excitability properties of neurons (Chen et al., 2006; Hsiao et al., 2009; Rossignol et al., 2013;
289 Specca et al., 2014). We therefore queried whether the effect of ATF4 on neuronal excitability was
290 in part due to its capability to regulate the expression or localization of K_v1.1, K_v2.1, K_v4.2, and
291 Ca_v2.1. As shown in Fig. 3B-E, neither the total nor the membrane-bound levels of these proteins
292 was affected by ATF4 down-regulation. These findings thus indicate that ATF4 has a selective
293 role in regulation of membrane-bound proteins involved in neuronal excitability and that this
294 includes GABA_BRs.

295 **ATF4 knockdown reduces GIRK currents**

296 We next queried whether the reduction we observed in the number of membrane-inserted
297 GABA_BRs after ATF4 down-regulation reflected a change in the functionality of the receptors
298 themselves. Post-synaptic GABA_BRs are associated with, and mediate part of their functions
299 through G protein-coupled inwardly-rectifying potassium (GIRK) channels (Gassmann and
300 Bettler, 2012). We therefore studied the function of GABA_BRs by whole-cell patch-clamp recording
301 of GABA_BR-induced K⁺ GIRK currents in 7 DIV hippocampal cultured neurons infected for 2 weeks
302 with lentiviruses carrying either shCtrl or shATF4. As shown in Fig. 4A, we first calibrated our
303 recordings by applying the GABA_BR agonist Baclofen (100 μ M), which elicited sustained K⁺
304 currents in control neurons that were prevented by pre-treating the cells with a specific GABA_BR
305 antagonist (SCH50911, 100 μ M). Consistent with our finding that ATF4 down-regulation reduces
306 cell surface GABA_BR levels, when we recorded Baclofen-induced GIRK currents in ATF4
307 knockdown neurons, we found them to be significantly reduced when compared to those in ShCtrl
308 infected neurons (Fig. 4B; shCtrl 725.9±58.4pA, shATF4 435.1±39.2pA; *post hoc* Bonferroni:
309 $p<0.01$). This effect did not appear to be mediated by effects on GIRK channels in that shATF4
310 did not affect total or membrane-bound GIRK1, GIRK2, or GIRK3 protein levels (Fig. 4C). Finally,
311 ATF4add, but not ATF4add/mut, completely restored the currents to the control level (Fig. 4B;
312 shATF4+ATF4add=786.9±69.2pA, shATF4+ATF4add/mut=545.9±43.8pA; *post hoc* Bonferroni:

313 shATF4 vs shATF4+ATF4add, $p<0.001$; shATF4add vs shATF4add/mut, $p<0.01$), further
314 confirming the idea that ATF4 needs to retain its transcriptional capability to regulate the trafficking
315 of GABA_BRs. As with GABA_BR membrane trafficking, ATF4 over-expression did not raise GIRK
316 current amplitude beyond that in control cultures.

317 **ATF4 knockdown increases the frequency, but not amplitude of mIPSCs**

318 Given that GABA_BR manipulations have been reported to affect the frequency, but not the
319 amplitude of spontaneous miniature inhibitory postsynaptic currents (mIPSCs; (Ulrich and
320 Huguenard, 1996; Kubota et al., 2003; Kirmse and Kirischuk, 2006)), we assessed mIPSCs
321 (confirmed by picrotoxin blockade) in cultured hippocampal neurons infected with either shCtrl or
322 shATF4 as a further readout of GABA_BR functionality. As shown in Figure 5A, we found that
323 shAT4 significantly increases (by about 2-fold) the frequency, but not the amplitude of mIPSCs
324 (mIPSCs frequency: shCtrl=1.65±0.21Hz, shATF4=3.43±0.41Hz; *post hoc* Bonferroni: $p<0.05$).
325 In addition, adding back ATF4 completely restored the frequency of mIPSCs to control values
326 (Fig. 5A; shATF4+ATF4add=1.19±0.37Hz; *post hoc* Bonferroni: shATF4 vs shATF4+ATF4add,
327 $p<0.05$). As with other properties described above, ATF4add overexpression did not increase
328 mIPSC frequency beyond the level observed in control cultures. Furthermore, our whole-cell
329 patch-clamp recordings showed that, unlike ATF4add, ATF4add/mut was unable to reverse the
330 effect of ATF4 down-regulation on mIPSC frequency (Fig. 5A;
331 shATF4+ATF4add/mut=3.83±0.76Hz; *post hoc* Bonferroni: shCtrl vs shATF4+ATF4add/mut,
332 $p<0.01$), confirming that the transcriptional activity of ATF4 is required for this action. To further
333 confirm the idea that membrane-bound GABA_BRs are reduced by shATF4, we treated both shCtrl
334 and shATF4-infected neurons with the specific GABA_BR agonist Baclofen (20 μM) or GABA_BR
335 antagonists SCH50911 and CGP55845 (used at 100 and 10 μM, respectively). As shown in Fig.
336 5B, Baclofen application significantly reduced the frequency of mIPSCs both in shCtrl- and
337 shATF4-infected hippocampal neurons (shCtrl+Baclofen=0.79±0.14Hz,
338 shATF4+Baclofen=1.23±0.15Hz; *post hoc* Bonferroni: shCtrl vs shCtrl+Baclofen, $p<0.05$; shATF4
339 vs shATF4+Baclofen, $p<0.01$), thus confirming that the membrane-bound GABA_BRs of shATF4-
340 infected hippocampal neurons are properly responding to stimulation. Interestingly, the
341 application of GABA_BR antagonists CGP55845 and SCH50911 significantly elevated mIPSCs
342 frequency in shCtrl but not in shATF4 neurons (Fig. 5B; shCtrl+SCH=3.19±0.30Hz,
343 shCtrl+CGP=3.67±0.46Hz, shATF4+SCH=3.38±0.44Hz, shATF4+CGP=3.59±0.15Hz; *post hoc*
344 Bonferroni: shCtrl vs shCtrl+SCH, $p<0.05$; shCtrl vs shCtrl+CGP, $p<0.05$, shATF4 vs
345 shATF4+SCH, shATF4 vs shATF4+CGP, $p>0.05$), which is consistent with the observation that
346 shATF4 reduces membrane-bound levels of GABA_BRs. As expected, none of the treatments
347 significantly affected the amplitude of mIPSCs (Fig. 5B).

348 **The effects of ATF4 on excitability and GABA_BRs appear to be mediated by changes in** 349 **Cdc42 expression**

350 We previously reported that ATF4's modulation of dendritic spine density and glutamatergic
351 functionality is mediated, at least in part, by its capacity to regulate the stability and expression of
352 the total and activated forms of the small Rho GTPase Cdc42 (Liu et al., 2014; Pasini et al., 2015).
353 Of particular relevance here, Cdc42 has been shown to be involved in regulating receptor

354 trafficking (Hussain et al., 2015). We therefore next tested the hypothesis that the effects of ATF4
355 down-regulation on GABA_BR trafficking and neuronal excitability could be mediated by loss of
356 Cdc42. To achieve this, we used a previously characterized Cdc42 shRNA (Liu et al., 2014) to
357 deplete Cdc42 in cultured hippocampal neurons and determined whether this phenocopies the
358 effects of ATF4 knockdown. We first assessed whether specific Cdc42 down-regulation affects
359 neuronal excitability. As in the case of ATF4 knockdown, silencing Cdc42 protein produced a 2-
360 fold increase of AP frequency (Fig. 6A; shCtrl=0.43±0.13Hz, shCdc42=1.08±0.15Hz; t test,
361 p<0.01). Next we queried whether Cdc42 down-regulation phenocopies the effect of ATF4
362 knockdown on GABA_BR trafficking and found that this was sufficient to significantly decrease the
363 levels of membrane-exposed, but not total GABA_BRs (Fig. 6B; for GABA_BR 1a
364 shCtrl=100%±23.3%, shCdc42 44.2%±7.4%; t test, p<0.05; GABA_BR 1b shCtrl=100%±20.3%,
365 shCdc42 38.7%±4.7%; t test, p<0.05). In addition, we found that Baclofen-induced GIRK currents
366 were significantly decreased in shCdc42-infected neurons, compared to controls (Fig. 6C;
367 shCtrl=627.8±77.6pA, shCdc42=406.9±52.9pA; t test, p<0.05). Finally, Cdc42 knockdown also
368 increased the frequency mIPSCs (Fig. 6D; shCtrl=1.55±0.16Hz, shCdc42=3.21±0.67Hz; t test,
369 p<0.05) to a degree similar to that observed with ATF4 knockdown. However, with Cdc42
370 knockdown, there was also a small, but significant increase in mIPSCs amplitude (Fig. 6D;
371 shCtrl=25.22±1.26pA, shCdc42=31±1.21pA; t test, p<0.01). Taken together, these findings
372 support the idea that regulation of Cdc42 levels mediates the effects of ATF4 on neuronal
373 GABA_BR trafficking and excitability.

374 Discussion

375 In the present study we delineate a novel role for the transcription factor ATF4 in regulating
376 GABA_BR trafficking and neuronal excitability. Our data show that chronic ATF4 down-regulation
377 in hippocampal neurons reduces membrane levels of GABA_BRs, diminishes their functionality,
378 and consequently leads to a substantial increase of neuronal firing rate. In addition, we found that
379 these effects are mediated by ATF4's transcriptional capability and reflect changes in expression
380 of the small GTPase Cdc42. Studies on ATF4's role in the regulation of synaptic plasticity and
381 memory have led to divergent views. ATF4 has been characterized to be either a negative or
382 positive influence on plasticity. Such interpretations appear to be dependent on cellular context
383 (Bartsch et al., 1995; Hu et al., 2015) or have been based on experimental manipulations that are
384 not specific to ATF4 such use of a dominant-negative construct (Chen et al., 2003) or regulation
385 of eIF2 α phosphorylation (Costa-Mattioli et al., 2007). To more directly assess ATF4's function in
386 unstressed brain, we have used the strategy of studying the effects of long-term ATF4 knockdown
387 or deletion in hippocampal and cortical neurons both *in vitro* and *in vivo*. This has revealed
388 required roles for ATF4 in maintaining mushroom spines and glutamatergic functionality as well
389 as in long-term spatial memory and behavioral flexibility (Liu et al., 2014; Pasini et al., 2015). The
390 present findings significantly extend the range of cognition-relevant neuronal properties that are
391 dependent on the presence of ATF4.

392 In the present work, we found that ATF4 plays a novel role in regulating the proportion of
393 GABA_BRs that are exposed on the neuronal surface. Two subunit isoforms of GABA_B 1 receptors
394 have been described, GABA_BR 1a and GABA_BR 1b, which differ by the presence of two sushi
395 domains near the N-terminus of GABA_BR 1a (Hawrot et al., 1998). Our findings indicate that ATF4

396 knockdown leads to comparable reductions of both GABA_BR 1a and GABA_BR 1b on the cell
397 surface. There is evidence that GABA_BR 1a subunits are mainly located presynaptically, while
398 GABA_BR 1b subunits are predominantly expressed postsynaptically (Vigot et al., 2006).
399 Consistent with this localization and with the reductions of both subunit types on the cell surface,
400 we observed both an increase in the frequency of mIPSCs (which is mainly a presynaptic
401 measurement) and a decrease of GIRK currents (mainly postsynaptic in origin) after ATF4
402 knockdown. Presynaptic GABA_BRs act as presynaptic brakes on release of neurotransmitters
403 (Sakaba and Neher, 2003; Laviv et al., 2010) and GABA_BR modulation consequently affects the
404 frequency, but not the amplitude, of mIPSCs (Ulrich and Huguenard, 1996; Kubota et al., 2003;
405 Kirmse and Kirischuk, 2006). Our observation that ATF4 down-regulation increases the
406 frequency, but not amplitude, of mIPSCs is thus consistent with a decrease of pre-synaptic
407 surface-exposed GABA_BRs. Further supporting this view, we found that application of the specific
408 GABA_BR antagonists CGP55845 and SCH50911 significantly elevated mIPSC frequency in
409 shCtrl- but not in shATF4-treated neurons, indicating that presynaptic GABA_BR activity is
410 compromised in the ATF4 knockdown neurons.

411 Pre- and post-synaptic GABA_BR function has been widely reported to be associated with G-
412 protein inward rectifying potassium channels (GIRKs), which hyperpolarize neurons in response
413 to GABA_BR activation (Ladera et al., 2008). We therefore measured GABA_BR-induced K⁺ currents
414 as a readout of GABA_BR activity and found a 40% reduction of GIRK current in ATF4 down-
415 regulated neurons. These observations are consistent with a decline in trafficking of post-synaptic
416 GABA_BRs. Thus, our findings suggest effects of ATF4 on both pre- and post-synaptic GABA_BRs.
417 Additional studies will be needed to further characterize these effects and to define their individual
418 influences on synaptic transmission.

419 In our study, we observed that the total and surface levels of GIRK proteins were unaltered by
420 ATF4 down-regulation; this finding suggests the idea that GABA_BRs and GIRK can be
421 independently trafficked to the cell surface. In addition, our finding that ATF4 down-regulation
422 reduces GABA_BR functionality without affecting GABA_BR 2 levels is in line with the evidence that
423 the 2 subunits (GABA_BR 1 and 2) need to heterodimerize in order to produce a functionally active
424 GABA_BR (Jones et al., 1998).

425 A major issue addressed in our study is the mechanism by which ATF4 regulates the surface
426 expression of GABA_BRs. As a leucine zipper protein, ATF4 has the capacity to undergo direct
427 protein-protein interactions, among which is binding to GABA_BRs. However, this interaction did
428 not appear to be relevant to the observed regulation of GABA_BR membrane trafficking since the
429 deficits in this parameter were not rescued by a mutant ATF4 lacking DNA binding capacity, but
430 possessing an intact leucine zipper. These observations support rather a transcriptional role for
431 ATF4 in regulating GABA_BR surface exposure. A prior study reported that ATF4 over-expression
432 elevated expression of a GABA_BR 1a promoter-reporter construct and decreased expression of a
433 GABA_BR 1b promoter-reporter construct (Steiger et al., 2004). However, we noted no changes
434 either in GABA_BR 1a or GABA_BR 1b mRNA or total protein after ATF4 knockdown. Moreover,
435 ATF4 over-expression also failed to affect surface or total GABA_BR 1a or GABA_BR 1b levels in
436 our experiments. Our findings instead indicate that the role of ATF4 in controlling GABA_BR
437 trafficking stems from its transcription-dependent capacity to regulate Cdc42 expression. In

438 support of this idea, Cdc42 knockdown fully phenocopied the effects of ATF4 knockdown on
439 surface expression of GABA_BRs. While the ATF4/Cdc42 pathway appears to be key player in
440 GABA_BR trafficking, this does not seem to be a universal mechanism for regulating receptor
441 surface expression in neurons. Thus, ATF4 knockdown did not affect total or membrane
442 expression of GABA_BR 2, GABA_A β2 and γ2 subunits, or K_v1.1, K_v2.1, K_v4.2, and Ca_v2.1 channels.
443 It remains to be seen whether ATF4/Cdc42 pathway affects trafficking of other neurotransmitter
444 receptors.

445 Cdc42-dependent signaling has been implicated in trafficking of GluA1 AMPA receptors (Hussain
446 et al., 2015). One way in which the effect of Cdc42 knockdown differed from ATF4 knockdown
447 was that the former, but not the latter caused a small, but significant increase in the amplitude of
448 mIPSCs. One possible explanation for this discrepancy may be the different magnitude of Cdc42
449 protein silencing exerted by the two shRNA constructs. While shATF4 caused a ~40-50%
450 reduction of Cdc42 protein, shCdc42 depleted 70-80% of total Cdc42 protein. It may be that the
451 greater loss of Cdc42 with shCdc42 results in post-synaptic modifications that affect GABA
452 sensitivity.

453 Our findings establish roles for transcriptionally active ATF4 and for Cdc42 in regulation of
454 GABA_BR trafficking. Our prior work has shown that ATF4 influences Cdc42 levels by promoting
455 its stability and that this in turn reflects the Cdc42-stabilizing activity of RhoGDIα, a direct
456 transcriptional target of ATF4 (Pasini et al., 2016). Fig. 7 shows a proposed mechanistic pathway
457 by which ATF4 regulates GABA_BR trafficking and neuronal excitability via Cdc42 and RhoGDIα.
458 An important feature of this mechanism is that it appears to occur over a prolonged time course.
459 Cdc42 is a relatively stable protein and knocking down ATF4 in neurons reduces Cdc42's
460 apparent half-life from 31.5 to 18.5 hrs (Liu et al., 2014). This suggests that sustained changes in
461 ATF4 protein levels/activity over many hours may be required to materially affect Cdc42
462 expression and thereby to affect synaptic activity. ATF4 itself is a rapidly turning-over protein and
463 its expression is regulated both by translational and transcriptional mechanisms. Thus ATF4 may
464 serve as a "sentinel" protein whose ambient expression levels in neurons influence GABA_BR
465 trafficking as well as other elements of neuronal plasticity.

466

467 **Figure Legends:**

468 **Figure 1:**

469 **ATF4 knockdown increases neuronal excitability. A,** The frequency of spontaneously-
470 occurring action potentials (sAPs) is increased upon ATF4 down-regulation; this effect appears
471 to be mediated by ATF4's transcriptional capability. Left panel, representative traces of sAPs
472 recorded from cultured hippocampal neurons infected at *DIV7* for 2 weeks with lentivirus
473 expressing either shCtrl (black trace), shATF4 (red trace), shATF4+ATF4add (purple trace), or
474 shATF4+ATF4add/mut (cyan trace). Right panel, summary bar graph showing the mean
475 frequencies (± SEM) of sAPs of hippocampal neurons infected with shCtrl (black bars, n=24),
476 shATF4 (red bars, n=22), shATF4+ATF4add (purple bars, n=18), shATF4+ATF4add/mut (cyan
477 bars, n=18) constructs. **C-E,** ATF4 down-regulation does not affect Na²⁺ and K⁺ voltage-gated

478 channels in shATF4-infected neurons (red dots) when compared to shCtrl neurons (black dots).
479 **C**, Voltage-gated Na²⁺ currents were evoked by 1s step depolarizations from -40 to +60 mV with
480 10-mV increments (shCtrl n=15; shATF4 n=16). **D**, A-type K⁺ currents were evoked by 1s step
481 depolarizations from -30 to +60 mV, with 10-mV increments (shCtrl n=29; shATF4 n=33), and
482 successively isolated. **E**, Delayed-rectifying K⁺ currents were evoked by 1s step depolarizations
483 from -90 to +60 mV, with 10 mV increments (shCtrl n=30; shATF4 n=34), and successively
484 isolated. Values are expressed as mean ± SEM. *p<0.05; **p<0.01.

485

486 **Figure 2:**

487 **ATF4 regulates GABA_BRs surface expression.** **A**, GABA_BR blockade increases the frequency
488 of sAPs in control neurons. Representative trace of sAPs recorded from cultured hippocampal
489 neurons infected with shCtrl-carrying lentivirus treated with the specific GABA_BR antagonist
490 CGP55845 (10 μM). **B**, Time-course experiment showing no changes in the mRNA levels for
491 GABA_BR subunits 1a and 1b upon ATF4 down-regulation. Bar graphs represent qPCR analysis
492 of ATF4 (left), GABA_BR 1a (center) and GABA_BR 1b (right) mRNA levels extracted 4, 8, and 12
493 days after infection with lentivirus carrying either shCtrl (black bars) or shATF4 (red bars)
494 constructs. Values are expressed as mean ± SEM from three independent experiments. **C**, ATF4
495 down-regulation decreases membrane levels of GABA_BR. *DIV7* hippocampal cultured neurons
496 were infected with indicated lentiviral constructs (black for shCtrl, red for shATF4, purple for
497 shATF4+ATF4add, and cyan for shATF4+ATF4add/mut) for 14 days before undergoing
498 extraction of total and membrane proteins. Left side of the panel shows a representative western
499 immunoblot. Bar graphs on the right portion of the panel show densitometric analysis of total (left)
500 or membrane (right) GABA_BR 1a and 1b protein normalized to GAPDH. **D**, ATF4 down-regulation
501 does not affect total or surface levels of GABA_BR 2. Left side of the panel shows a representative
502 western immunoblot. Bar graphs on the right portion of the panel show densitometric analysis of
503 total (left) or membrane (right) GABA_BR 2 protein normalized to GAPDH. Values are expressed
504 as mean ± SEM from three independent experiments. *p<0.05. **p<0.01; ***p<0.001.

505

506 **Figure 3:**

507 **ATF4 down-regulation does not affect total and membrane levels of GABA_ARs and voltage-**
508 **sensitive K or Ca channels.** *DIV7* cultured hippocampal neurons were infected with indicated
509 lentiviral constructs (black for shCtrl, red for shATF4) for 14 days before undergoing extraction of
510 total and membrane proteins. **A**, Left side of the panel shows a representative western
511 immunoblot. Bar graphs show densitometric analysis of total (left) or membrane (right) GABA_AR
512 β2 and γ2 protein normalized to GAPDH. **B**, Upper panel shows a representative western
513 immunoblot. Bar graphs show densitometric analysis of total (left) or membrane (right) K_v1.1
514 protein normalized to GAPDH. **C**, Upper panel shows a representative western immunoblot. Bar
515 graphs show densitometric analysis of total (left) or membrane (right) K_v2.1 protein normalized to
516 GAPDH. **D**, Upper panel shows a representative western immunoblot. Bar graphs show
517 densitometric analysis of total (left) or membrane (right) K_v4.2 protein normalized to GAPDH. **E**,

518 Upper panel shows a representative western immunoblot. Bar graphs show densitometric
519 analysis of total (left) or membrane (right) $\text{Ca}_v2.1$ protein normalized to GAPDH. Values are
520 expressed as mean \pm SEM from three independent experiments, each run in duplicate. The
521 differences between shCtrl and shATF4 were not significant ($p>0.05$) in all cases.

522

523 **Figure 4:**

524 **ATF4 knockdown reduces GABA_BR-induced GIRK currents.** **A,** Specific GABA_BR agonist
525 Baclofen (100 μM) elicited a sustained GIRK current in cultured hippocampal neurons infected
526 with shCtrl lentivirus (top panel shows a representative trace). This effect is abolished by
527 pretreating the culture with the specific GABA_BR antagonist CGP55845 (10 μM ; bottom panel).
528 **B,** shATF4 infection reduces Baclofen-induced GIRK currents; this effect is dependent on ATF4's
529 transcriptional capability. Left panel shows representative traces of Baclofen-elicited currents
530 recorded from *DIV7* cultured hippocampal neurons infected for two weeks with lentivirus
531 expressing either shCtrl (black), shATF4 (red), shATF4+ATF4add (purple), or
532 shATF4+ATF4add/mut (cyan). Bar graphs on the right indicate measurements of the currents
533 (shCtrl n=37; shATF4 n=39; shATF4+ATF4add n=36; shATF4+ATF4add/mut n=51). Values are
534 expressed as mean \pm SEM. * $p<0.05$; ** $p<0.005$. **C,** ATF4 down-regulation does not affect total
535 and membrane levels of GIRK proteins. *DIV7* cultured hippocampal neurons were infected with
536 indicated lentiviral constructs (black for shCtrl, red for shATF4) for 14 days before undergoing
537 extraction of total and membrane proteins. Left side of the panel shows a representative western
538 immunoblot. Bar graphs show densitometric analysis of total (left) or membrane (right) GIRK
539 proteins normalized to GAPDH. Values are expressed as mean \pm SEM from three independent
540 experiments. * $p<0.05$. ** $p<0.01$; *** $p<0.001$.

541

542 **Figure 5:**

543 **ATF4 knockdown increases the frequency, but not amplitude of mIPSCs.** **A,** Left portion of
544 the panel shows representative mIPSC traces recorded from *DIV7* hippocampal neurons infected
545 for two weeks with lentivirus expressing either shCtrl (black), shATF4 (red), shATF4+ATF4add
546 (purple), or shATF4+ATF4add/mut (cyan). On the right portion of the panel, bar graphs quantify
547 the frequency (left) and the amplitude (right) of mIPSCs shown in A. (shCtrl, n=46; shATF4, n=29;
548 shATF4+ATF4add, n=16; shATF4+ATF4add/mut, n=25). Values are expressed as mean \pm SEM.
549 **B,** Effect of pharmacological manipulation of GABA_BR on mIPSCs recorded from *DIV7*
550 hippocampal neurons infected for two weeks with lentivirus expressing either shCtrl, or shATF4.
551 Top panel shows representative traces of mIPSCs recorded from shCtrl (black traces) or shATF4
552 (red traces) infected neurons alone (shCtrl, n=49; shATF4, n=29) or in the presence of either 20
553 μM Baclofen (GABA_BR agonist; shCtrl, n=16; shATF4, n=15), 10 μM SCH50911 (GABA_BR
554 antagonist; shCtrl, n=36; shATF4, n=18), or 100 μM CGP55845 (GABA_BR antagonist; shCtrl,
555 n=21; shATF4, n=17). In the bottom portion of the panel, bar graphs quantify the frequency (left)
556 and the amplitude (right) of the mIPSCs. Values are expressed as mean \pm SEM. * indicates
557 $p<0.05$; ** indicates $p<0.01$; *** indicates $p<0.001$.

558

559 **Figure 6:**

560 **The effects of ATF4 on excitability and GABA_BRs are driven by changes in Cdc42**
561 **expression. A,** Cdc42 down-regulation increases intrinsic neuronal excitability. Top panel shows
562 representative traces of sAPs recorded from cultured hippocampal neurons infected at *DIV7* for
563 2 weeks with lentivirus expressing either shCtrl (black trace) or shCdc42 (blue trace). Bottom
564 panel shows summary bar graphs showing the frequency of sAPs of neurons infected with shCtrl
565 (black bars, n=13) or shCdc42 (blue bars, n=13) constructs. **B,** Cdc42 down-regulation decreases
566 membrane but not total GABA_BR levels. *DIV7* cultured hippocampal neurons were infected with
567 different lentiviral constructs (black for shCtrl, blue for shCdc42) for two weeks before undergoing
568 extraction of total and membrane proteins. Left portion of the panel shows a representative
569 Western immunoblot. Bar graphs on the right portion of the panel show densitometric analysis of
570 immunoblots for total (left) or membrane (right) GABA_BR 1a and 1b protein, normalized to
571 GAPDH. **C,** Cdc42 down-regulation decreases Baclofen-elicited GIRK currents. Top side of the
572 panel shows representative traces of Baclofen-elicited currents recorded from *DIV7* cultured
573 hippocampal neurons infected for two weeks with lentivirus carrying either shCtrl (black) or
574 shCdc42 (blue). Bar graph on the bottom side shows the measurements of the currents (shCtrl,
575 n=22; shCdc42, n=26). **D,** Cdc42 down-regulation increases mIPSCs. Top portion of the panel
576 shows representative mIPSC traces recorded from *DIV7* hippocampal neurons infected for two
577 weeks with lentivirus carrying either shCtrl (black) or shCdc42 (blue) constructs. On the bottom
578 portion of the panel, bar graphs quantify the frequency (left) and the amplitude (right) of mIPSCs
579 shown in A. (shCtrl, n=34; shCdc42, n=29). Values are expressed as mean ± SEM. * indicates
580 p<0.05.

581

582 **Figure 7:**

583 **Proposed mechanism by which ATF4 regulates neuronal excitability.** Left panel shows a
584 control condition where basal levels of ATF4 protein ensure the appropriate amount of RhoGDI α
585 expression to bind and stabilize cytoplasmic Rho GTPase family members, including Cdc42.
586 Appropriate levels of Cdc42 result in basal levels of membrane-bound GABA_BRs that contribute
587 to control the pace of neuronal firing. The right side of the panel shows a condition of chronic
588 ATF4 down regulation, the consequent decrease of RhoGDI α levels and augmented Cdc42
589 turnover. This in turn negatively affects the amount of membrane-bound GABA_BRs, altering
590 neuronal intrinsic excitability properties, which results in increased sAP frequency.

591

592 **References:**

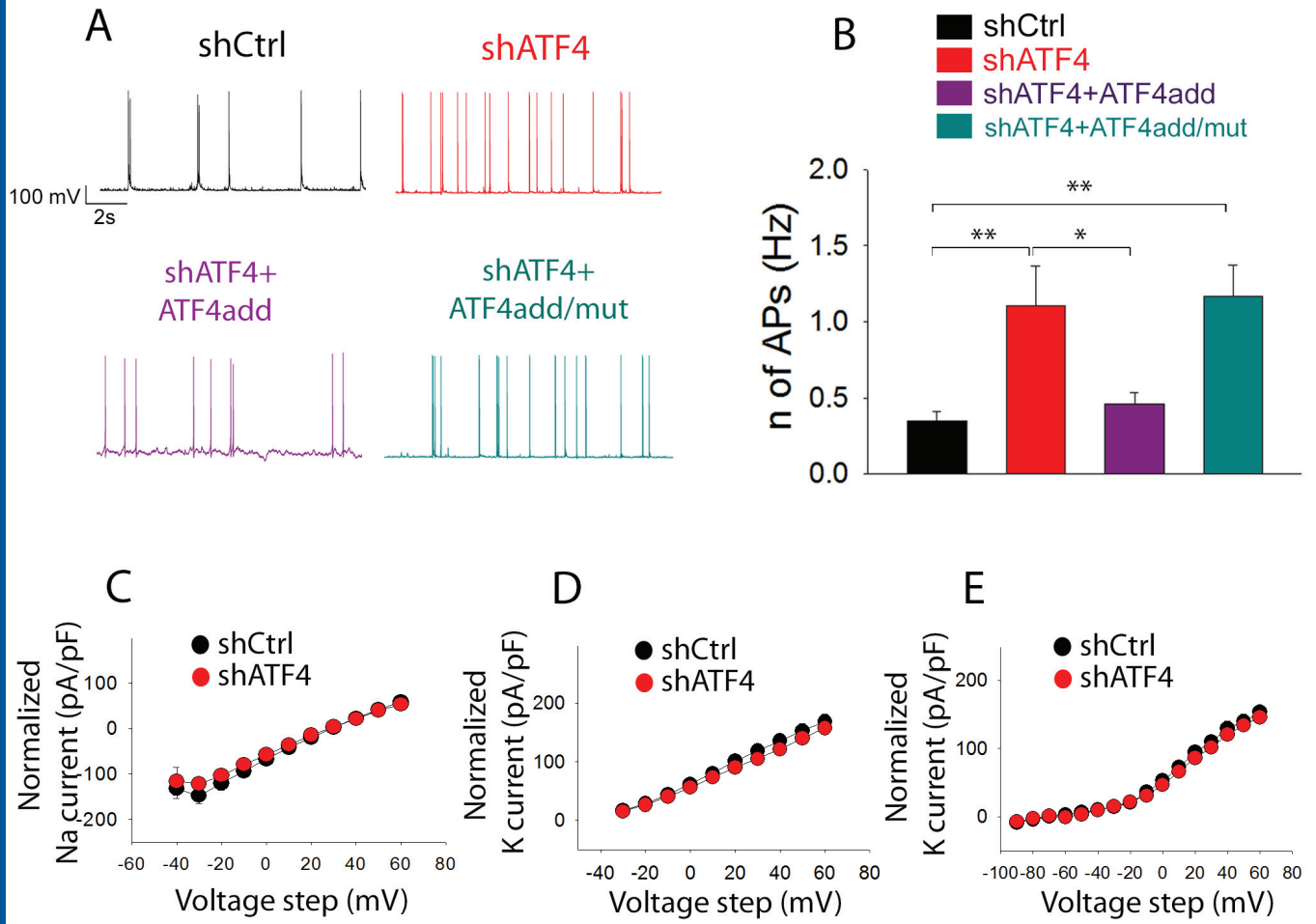
593

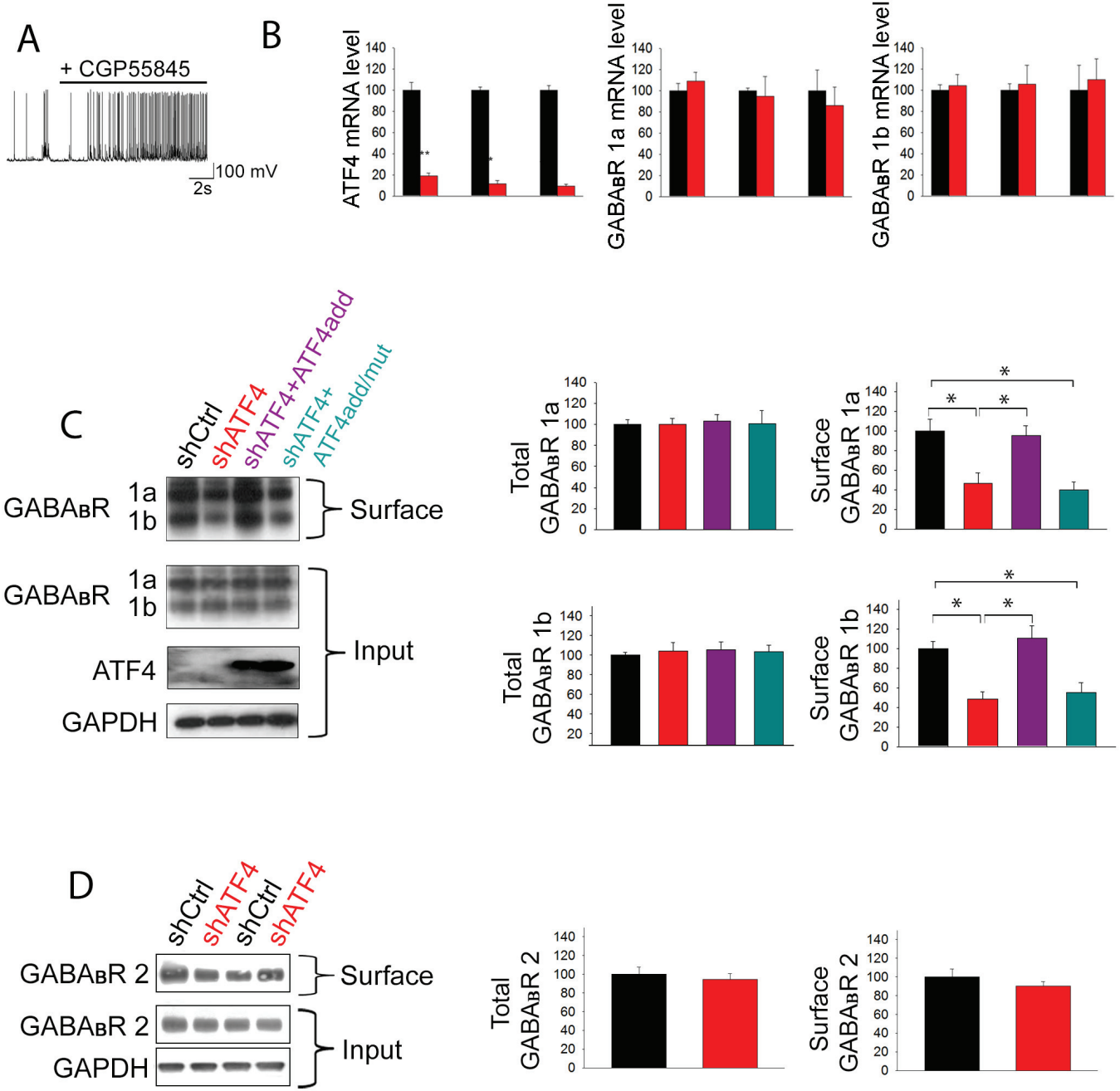
594 Ameri K, Harris AL (2008) Activating transcription factor 4. *Int J Biochem Cell Biol* 40:14-21.

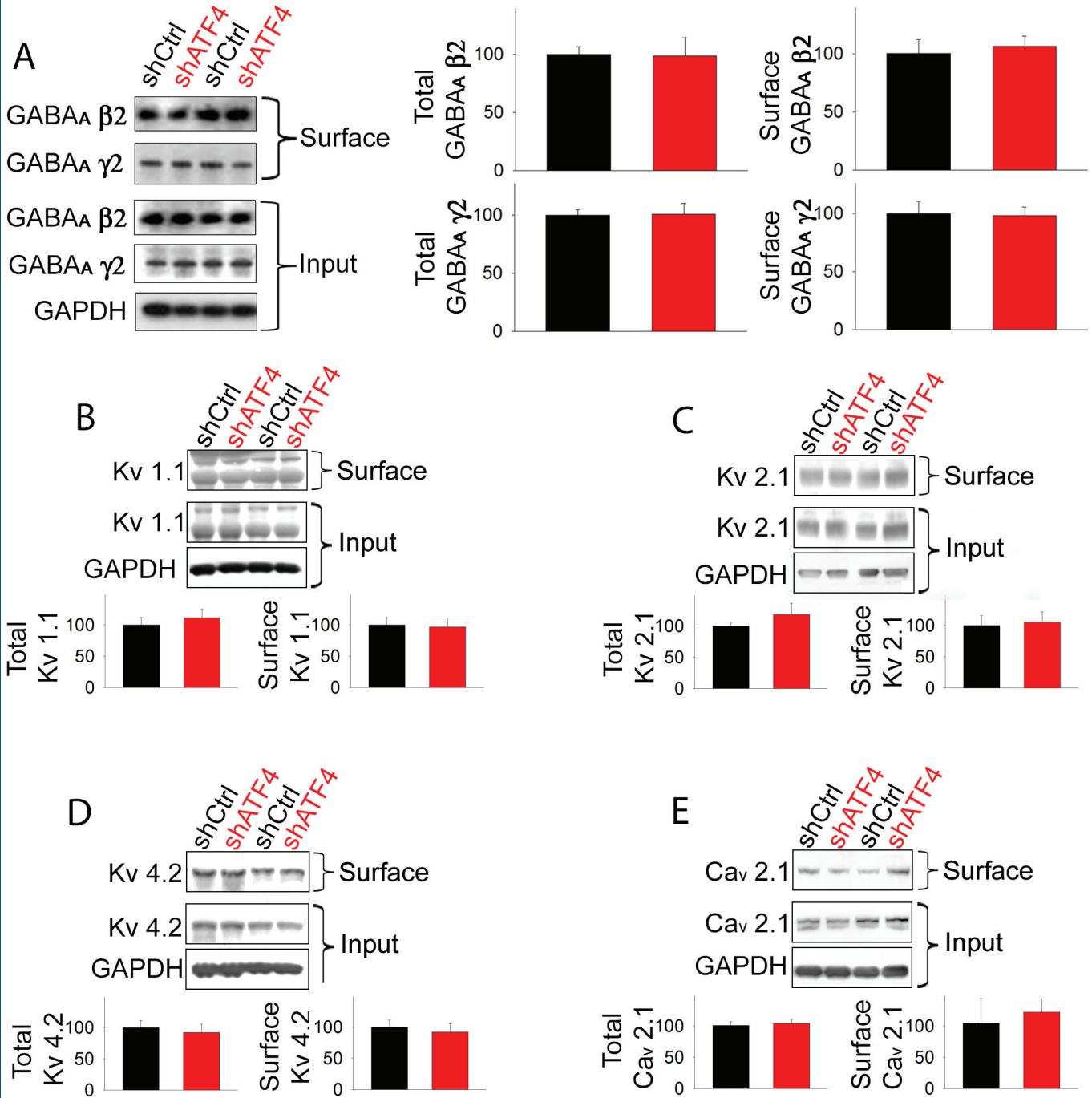
- 595 Bartsch D, Ghirardi M, Skehel PA, Karl KA, Herder SP, Chen M, Bailey CH, Kandel ER (1995) Aplysia CREB2
596 represses long-term facilitation: relief of repression converts transient facilitation into long-term
597 functional and structural change. *Cell* 83:979-992.
- 598 Bean BP (2007) The action potential in mammalian central neurons. *Nat Rev Neurosci* 8:451-465.
- 599 Beck H, Yaari Y (2008) Plasticity of intrinsic neuronal properties in CNS disorders. *Nat Rev Neurosci*
600 9:357-369.
- 601 Chen A, Muzzio IA, Malleret G, Bartsch D, Verbitsky M, Pavlidis P, Yonan AL, Vronskaya S, Grody MB,
602 Cepeda I, Gilliam TC, Kandel ER (2003) Inducible enhancement of memory storage and synaptic
603 plasticity in transgenic mice expressing an inhibitor of ATF4 (CREB-2) and C/EBP proteins.
604 *Neuron* 39:655-669.
- 605 Chen X, Yuan LL, Zhao C, Birnbaum SG, Frick A, Jung WE, Schwarz TL, Sweatt JD, Johnston D (2006)
606 Deletion of Kv4.2 gene eliminates dendritic A-type K⁺ current and enhances induction of long-
607 term potentiation in hippocampal CA1 pyramidal neurons. *J Neurosci* 26:12143-12151.
- 608 Costa-Mattioli M, Gobert D, Stern E, Gamache K, Colina R, Cuellar C, Sossin W, Kaufman R, Pelletier J,
609 Rosenblum K, Krnjevic K, Lacaille JC, Nader K, Sonenberg N (2007) eIF2 α phosphorylation
610 bidirectionally regulates the switch from short- to long-term synaptic plasticity and memory. *Cell*
611 129:195-206.
- 612 Gassmann M, Bettler B (2012) Regulation of neuronal GABA(B) receptor functions by subunit
613 composition. *Nat Rev Neurosci* 13:380-394.
- 614 Hawrot E, Xiao Y, Shi QL, Norman D, Kirkitadze M, Barlow PN (1998) Demonstration of a tandem pair of
615 complement protein modules in GABA(B) receptor 1a. *FEBS Lett* 432:103-108.
- 616 Hsiao CF, Kaur G, Vong A, Bawa H, Chandler SH (2009) Participation of Kv1 channels in control of
617 membrane excitability and burst generation in mesencephalic V neurons. *J Neurophysiol*
618 101:1407-1418.
- 619 Hu JY, Levine A, Sung YJ, Schacher S (2015) cJun and CREB2 in the postsynaptic neuron contribute to
620 persistent long-term facilitation at a behaviorally relevant synapse. *J Neurosci* 35:386-395.
- 621 Hussain NK, Thomas GM, Luo J, Huganir RL (2015) Regulation of AMPA receptor subunit GluA1 surface
622 expression by PAK3 phosphorylation. *Proc Natl Acad Sci U S A* 112:E5883-5890.
- 623 Jones KA, Borowsky B, Tamm JA, Craig DA, Durkin MM, Dai M, Yao WJ, Johnson M, Gunwaldsen C,
624 Huang LY, Tang C, Shen Q, Salon JA, Morse K, Laz T, Smith KE, Nagarathnam D, Noble SA,
625 Branchek TA, Gerald C (1998) GABA(B) receptors function as a heteromeric assembly of the
626 subunits GABA(B)R1 and GABA(B)R2. *Nature* 396:674-679.
- 627 Kim IH, Wang H, Soderling SH, Yasuda R (2014) Loss of Cdc42 leads to defects in synaptic plasticity and
628 remote memory recall. *Elife* 3.
- 629 Kirmse K, Kirischuk S (2006) Ambient GABA constrains the strength of GABAergic synapses at Cajal-
630 Retzius cells in the developing visual cortex. *J Neurosci* 26:4216-4227.
- 631 Kubota H, Katsurabayashi S, Moorhouse AJ, Murakami N, Koga H, Akaike N (2003) GABAB receptor
632 transduction mechanisms, and cross-talk between protein kinases A and C, in GABAergic
633 terminals synapsing onto neurons of the rat nucleus basalis of Meynert. *J Physiol* 551:263-276.
- 634 Ladera C, del Carmen Godino M, Jose Cabanero M, Torres M, Watanabe M, Lujan R, Sanchez-Prieto J
635 (2008) Pre-synaptic GABA receptors inhibit glutamate release through GIRK channels in rat
636 cerebral cortex. *J Neurochem* 107:1506-1517.
- 637 Laviv T, Riven I, Dolev I, Vertkin I, Balana B, Slesinger PA, Slutsky I (2010) Basal GABA regulates GABA(B)R
638 conformation and release probability at single hippocampal synapses. *Neuron* 67:253-267.
- 639 Leung LS, Peloquin P (2006) GABA(B) receptors inhibit backpropagating dendritic spikes in hippocampal
640 CA1 pyramidal cells in vivo. *Hippocampus* 16:388-407.
- 641 Liu J, Pasini S, Shelanski ML, Greene LA (2014) Activating transcription factor 4 (ATF4) modulates post-
642 synaptic development and dendritic spine morphology. *Front Cell Neurosci* 8:177.

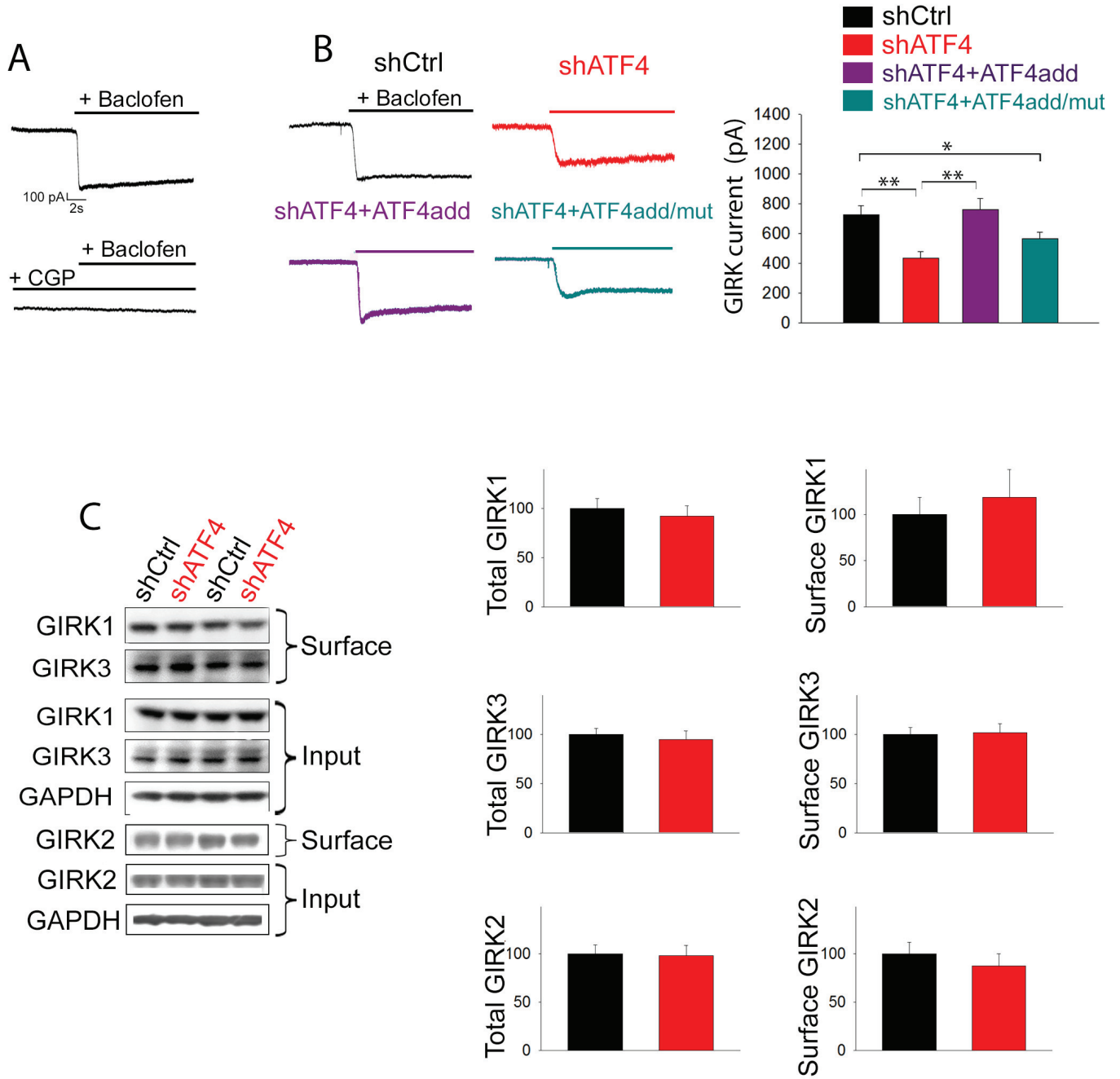
- 643 Nehring RB, Horikawa HP, El Far O, Kneussel M, Brandstatter JH, Stamm S, Wischmeyer E, Betz H,
644 Karschin A (2000) The metabotropic GABAB receptor directly interacts with the activating
645 transcription factor 4. *J Biol Chem* 275:35185-35191.
- 646 Pasini S, Corona C, Liu J, Greene LA, Shelanski ML (2015) Specific downregulation of hippocampal ATF4
647 reveals a necessary role in synaptic plasticity and memory. *Cell Rep* 11:183-191.
- 648 Pasini S, Liu J, Corona C, Peze-Heidsieck E, Shelanski M, Greene LA (2016) Activating Transcription Factor
649 4 (ATF4) modulates Rho GTPase levels and function via regulation of RhoGDIalpha. *Sci Rep*
650 6:36952.
- 651 Ritter B, Zschuntsch J, Kvachnina E, Zhang W, Ponimaskin EG (2004) The GABA(B) receptor subunits R1
652 and R2 interact differentially with the activation transcription factor ATF4 in mouse brain during
653 the postnatal development. *Brain Res Dev Brain Res* 149:73-77.
- 654 Rossignol E, Kruglikov I, van den Maagdenberg AM, Rudy B, Fishell G (2013) CaV 2.1 ablation in cortical
655 interneurons selectively impairs fast-spiking basket cells and causes generalized seizures. *Ann*
656 *Neurol* 74:209-222.
- 657 Sakaba T, Neher E (2003) Direct modulation of synaptic vesicle priming by GABA(B) receptor activation
658 at a glutamatergic synapse. *Nature* 424:775-778.
- 659 Speca DJ, Ogata G, Mandikian D, Bishop HI, Wiler SW, Eum K, Wenzel HJ, Doisy ET, Matt L, Campi KL,
660 Golub MS, Nerbonne JM, Hell JW, Trainor BC, Sack JT, Schwartzkroin PA, Trimmer JS (2014)
661 Deletion of the Kv2.1 delayed rectifier potassium channel leads to neuronal and behavioral
662 hyperexcitability. *Genes Brain Behav* 13:394-408.
- 663 Steiger JL, Bandyopadhyay S, Farb DH, Russek SJ (2004) cAMP response element-binding protein,
664 activating transcription factor-4, and upstream stimulatory factor differentially control
665 hippocampal GABABR1a and GABABR1b subunit gene expression through alternative
666 promoters. *J Neurosci* 24:6115-6126.
- 667 Ulrich D, Huguenard JR (1996) Gamma-aminobutyric acid type B receptor-dependent burst-firing in
668 thalamic neurons: a dynamic clamp study. *Proc Natl Acad Sci U S A* 93:13245-13249.
- 669 Vernon E, Meyer G, Pickard L, Dev K, Molnar E, Collingridge GL, Henley JM (2001) GABA(B) receptors
670 couple directly to the transcription factor ATF4. *Mol Cell Neurosci* 17:637-645.
- 671 Vigot R, Barbieri S, Brauner-Osborne H, Turecek R, Shigemoto R, Zhang YP, Lujan R, Jacobson LH,
672 Biermann B, Fritschy JM, Vacher CM, Muller M, Sansig G, Guetg N, Cryan JF, Kaupmann K,
673 Gassmann M, Oertner TG, Bettler B (2006) Differential compartmentalization and distinct
674 functions of GABAB receptor variants. *Neuron* 50:589-601.
- 675 White JH, McIlhinney RA, Wise A, Ciruela F, Chan WY, Emson PC, Billinton A, Marshall FH (2000) The
676 GABAB receptor interacts directly with the related transcription factors CREB2 and ATFx. *Proc*
677 *Natl Acad Sci U S A* 97:13967-13972.
- 678 Zapata J et al. (2017) Epilepsy and intellectual disability linked protein Shrm4 interaction with GABABRs
679 shapes inhibitory neurotransmission. *Nat Commun* 8:14536.

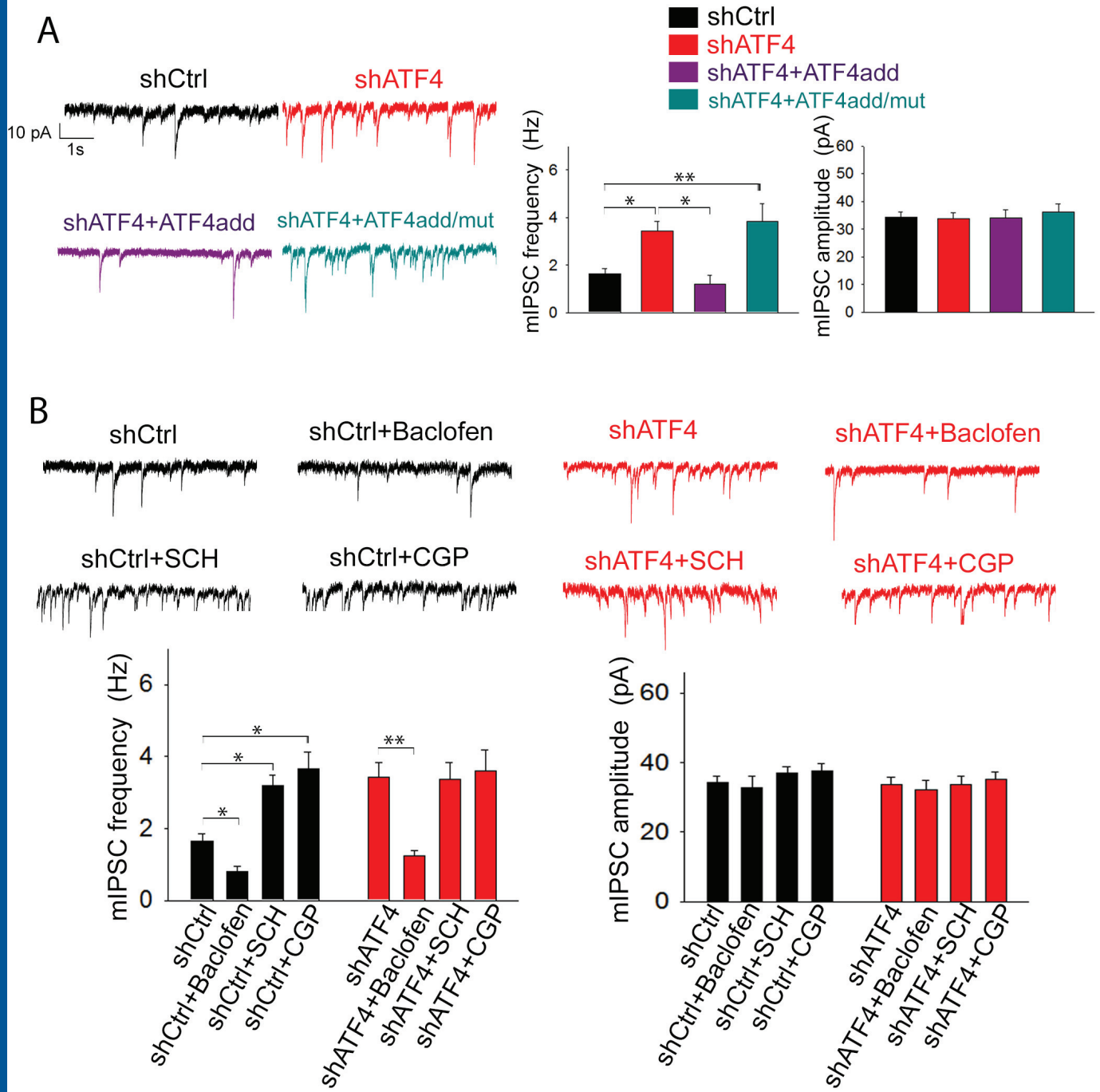
680

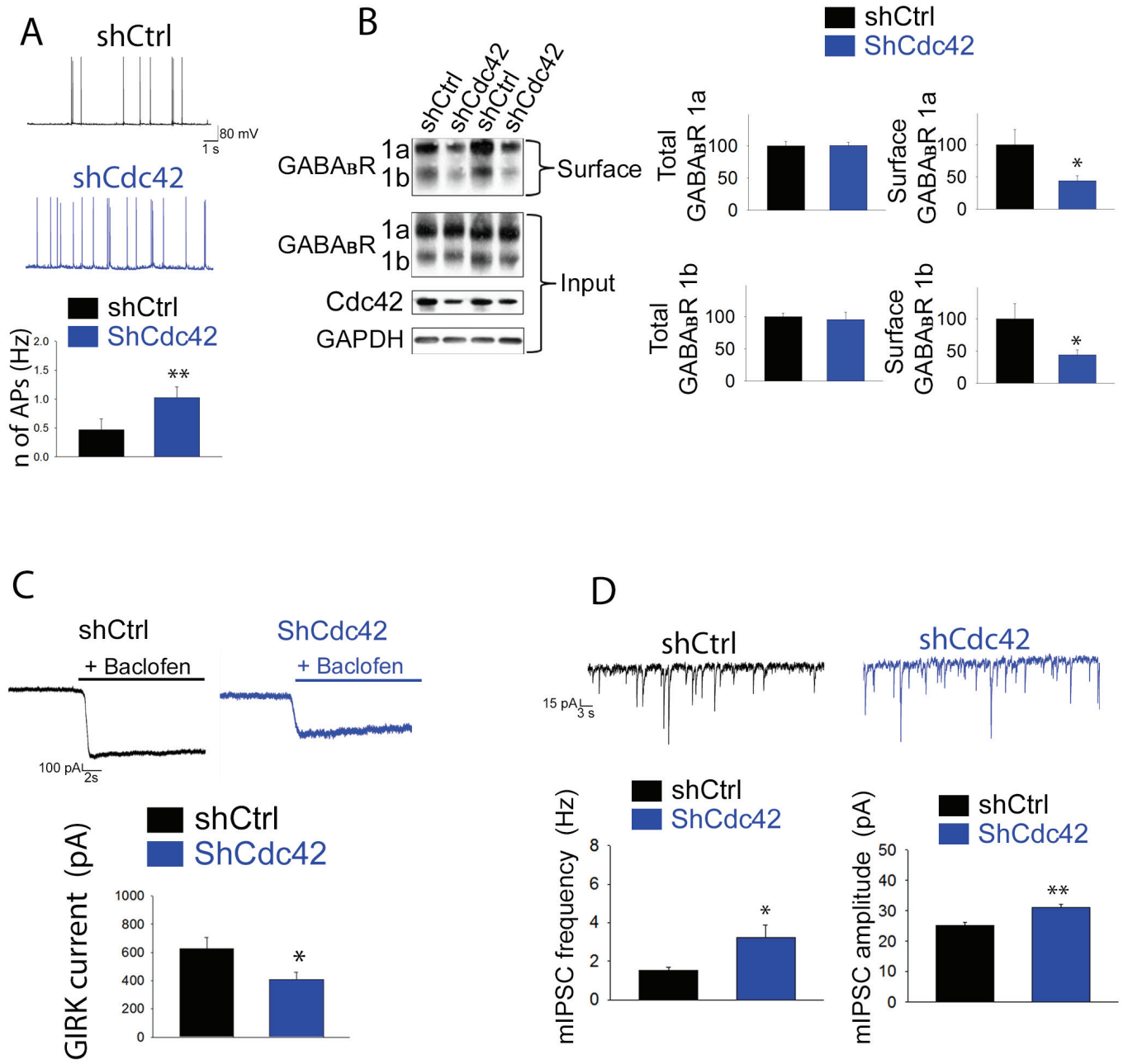




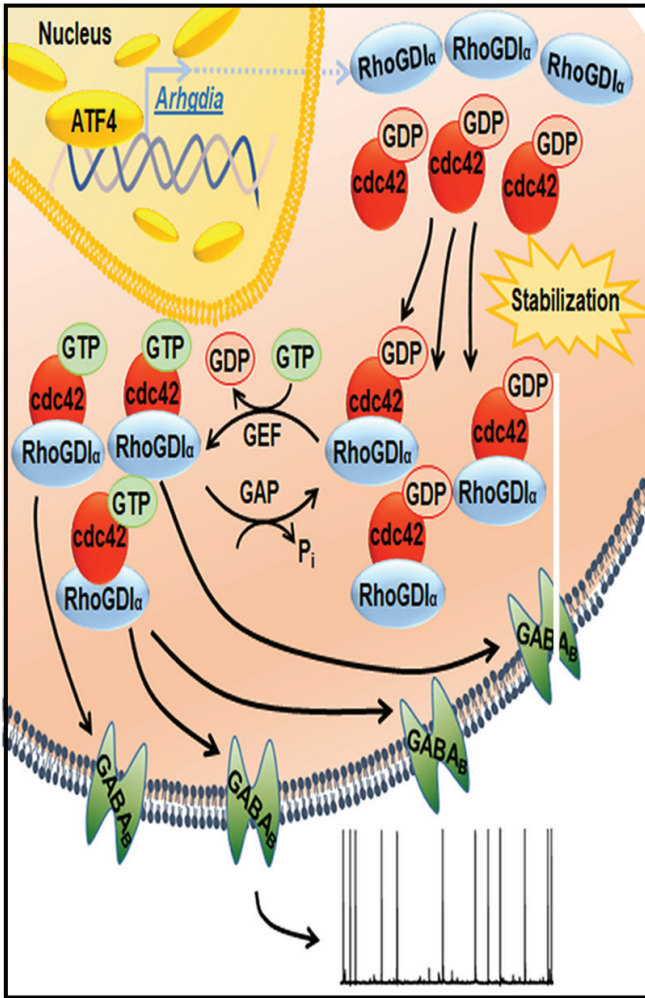








Control



Chronic ATF4 down-regulation

